



Fluorescence strobo-stereoscopy for specular reflection-suppressed full field of view imaging

Xiangyu Guo, ChaBum Lee ^{*}

J. Mike Walker '66 Department of Mechanical Engineering, Texas A&M University, 3123 TAMU, College Station, TX 77843-3123, USA

ARTICLE INFO

Keywords:

Fluorescence strobo-stereoscopy

Specular reflection

3D surface imaging

Surface quality

ABSTRACT

This paper introduces fluorescence strobo-stereoscopy (FSS) to suppress strong specular reflection and enable the full field of view (FFOV) 3D surface imaging while the part is rotating. Specular reflection off the target surface significantly degrades the image quality and becomes critical for highly reflective surface measurements. In FSS, the fluorescent dye-doped fluid applied on the machined surface is excited upon incident ultra-violet light and becomes a new light source by Stokes' Law. Thus, specular reflection off of smooth surface can be suppressed by separating the fluorescent light from the excitation light. The developed FSS comprises a pair of imaging cameras, spatial filters, and an excitation light source. As a result, FSS effectively rejected the specular reflection and improved the FFOV 3D surface image quality of the machined part by enhancing contrast in the rotating target surface. Such enhancements in 3D imaging allowed to identify manufacturing tolerance of the part and to detect the surface features. The axial and lateral accuracy errors of FSS were 2.3% and 1.4% with the target size of 4.07 mm and 0.215 mm, respectively. A whole view reconstruction of the cylindrical target sample was performed, and the corresponding cylindricity and diameter deviation were assessed. The fluid media effect and the target surface quality effect were discussed.

1. Introduction

Stereoscopy is a 3D imaging technique for adding the illusion of image depth to two surface images captured by a pair of vision camera units, and measures shape, displacement, deformation of the measurement target surfaces [1–5]. The measurement accuracy and precision of stereoscopy are determined by the performance of vision cameras such as pixel size, focusing lenses, frame rate, and so on. However, stereoscopy is limited to the highly reflective surface measurement where specular reflection exists on the smooth surface known as glare, which causes a lack of information on the directional reflection area and reduces the brightness and contrast of the rest of the scanning area [5,6]. So, strong specular reflection in the imaging systems causes strong highlights in the imaging devices and results in surface information loss. Many pieces of researches have been conducted to characterize and remove specular reflection problems using color, polarization, multiple views, and multi-flashing [1–9]. Those methods are primarily focused on imaging systems and display devices such as lenses, back-light units, glasses, or optical films. Recently, efforts to increase the measurement resolution and enhance imaging quality through scattering media such

as fluorescence dye-doped fluids were introduced [10–13]. However, those methods are limited to stationary target surface measurements or slow dynamic motion and deformation measurements.

This paper introduces an enhanced in-process 3D surface scanning method for a rotating target with excellent surface quality. Guo et al. recently introduced strobo-stereoscopy (SS) that can *in situ* reconstruct the 3D surface images of the cutting tool and rolling pin while rotating [14]. This method was limited to the 3D surface imaging of the highly reflective surface due to strong specular reflection off of the target surface, so the dark paint had to be applied on the target surface to mitigate specular reflection. However, such a surface condition modification could not ultimately solve the specular reflection problems. Here, the green fluorescence dye-doped fluid was used to suppress strong specular reflection, and the full field of imaging of a target surface rotating was in-process obtained by fluorescence strobo-stereoscopy (FSS).

2. Measurement principle

The fluorescent dye has two intrinsic characteristics. One is the Stokes shift, which occurs when the dye is activated by a certain

* Corresponding author.

E-mail address: cblee@tamu.edu (C. Lee).

ultraviolet (UV) light. Its emission wavelength is shifted and does not overlap with the excitation wavelength. When the fluorescent liquid is applied to the surface, its emitted direction is random. Thus, along with the band-pass filter, specular reflection from the excitation wavelength can be separated. The other advantage is the ability to increase speckle contrast, which helps improve reconstruction accuracy for the presence of more reference matching points in the pair of images.

Prior to the measurement, the fluorescent fluid was chosen as the mixture of Pylakrome LX-10215 particles (from Pylam Company) and fluorescent fluid PAG 150 oil. The excitation wavelength of the light-emitting diode (LED) light source was chosen as 365 nm and the emission wavelength measured by the spectrometer was 520 nm (central peak value) as seen in Fig. 1.

The experiment setting and the proposed FSS method were depicted in Fig. 2 (a). A pair of charge-coupled device (CCD) cameras were employed for the image capturing, a 365 nm ($\lambda_{\text{excitation}}$) UV light was prepared for the excitation light source, a pair of high-pass filters (BPF > 370 nm) were chosen from the emission wavelength 520 nm ($\lambda_{\text{emission}}$) of the fluorescent fluid, and a rotary spindle was used for the target rotation. Using the fluorescent fluid can remove the sensitivity of the illumination system while highlighting the contrast, hence increasing the number of reference points, and the fluorescent fluid is sprayed to the surface in a spray bottle while the target sample is rotating. To show the advantage of the fluorescent fluid in eliminating specular reflections, a comparative result of reconstructing a 3D surface with the machined aluminum rod ($\phi 1''$) is shown in Fig. 2(b), showing that the fluorescent liquid can improve the optical quality-surface map reconstruction ability.

3. Measurement experiment

In this section, in order to test the effectiveness of the FSS, the fluid effect is discussed first. It appears that a higher viscosity fluid on the surface can reduce the specular effect. Comparison experiments on the targets with a rough surface and a polished surface were conducted between normal LED conditions and UV light conditions with fluorescent fluid. These results prove that the fluorescent fluid is capable of reconstructing the specular effect that existed on the surface. After this, the patterned structure target was measured to first track the FSS single image reconstruction ability on the pattern recognition, second to demonstrate the whole view reconstruction process. Finally, the cylindricity and roundness on the reconstructed 3D target were compared with the baseline data obtained by using the coordinate measuring machine (CMM) at Zeiss. All the samples are cylinder structures ($\phi 1''$).

3.1. Fluid media effects

To test the fluid media effect on the well-machined surface, stereoscopic experiments were constructed. The three different mediums (air, water, lubricant liquid) were applied to the polished cylinder. The reconstructed images in the framed area are shown in Fig. 3.

According to the results above, the liquid-applied casings can collect information about the blank area caused by the specular effect. In comparison to the other two situations, the lubricant liquid-coated surface diffuses the most specular light. This is illustrated by the findings of the framed area surface map, which shows that the lubricant-liquid-coated surface is capable of reconstructing the complete surface map while being least affected by specular light. The water condition of the framed area surface map is not lacking information; yet, the non-continuous strokes along the specular light area demonstrate that such a rebuilt surface is impacted by the light distribution. The results indicated that the general liquid can assist reduce the specular effect, and that liquids with a higher viscosity result in a smoother surface quality. In the camera view of Fig. 3, the tool mark, however, is the least clear in the lubricant case and less clear in the water case compared with the air case. This can also be proved by the surface map, as fewer structures exist in the media-introduced case. Thus, the scattering effect from the general liquid helps reduce the directional reflection intensity. The viscosity value is critical as it affects the quality of the surface reconstruction. However, such liquids can result in a blur or even a halo on the surface as it reduces the contrast at the same time. As a result, we proposed applying the fluorescent media to directly remove the specular effect without introducing irrelevant environmental noises. Fluorescent liquid absorbs the incident wavelength and converts it to another. By employing a bandpass filter, it is possible to minimize directional reflections while maintaining or even increasing the target area contrast.

3.2. Surface quality effects under FSS methods comparison

Rough surface quality and the polished surface on the Al cylinder quality are compared in this session. Fig. 4 presents the surface reconstruction results on the red-framed area. The center line extraction along the vertical direction is also presented in Fig. 4, the tendency on the linear results are similar. Based on the ASME B46.1-2019 [15], arithmetic average Ra value, can be calculated by the absolute values of the profile height deviations from the mean line is also calculated.

The Ra values measured on the normal LED and the fluorescent liquid cases for the polished surface case are 0.78 μm and 0.8 μm , respectively, and the direct difference ratio is 2.6%. Even though this difference is slight, the reconstruction ability under the normal LED case is limited due to the blank section. This is because of the specular light effect. For the rough surface, the measured results are 1.02 μm and 0.98

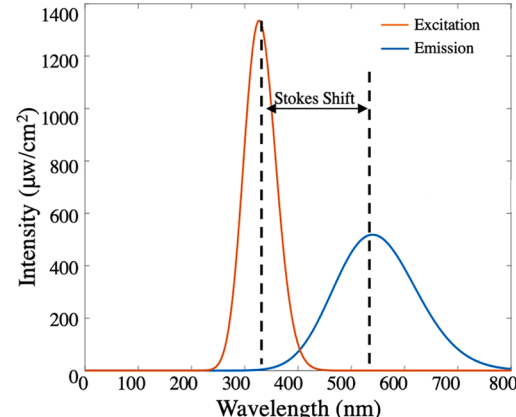
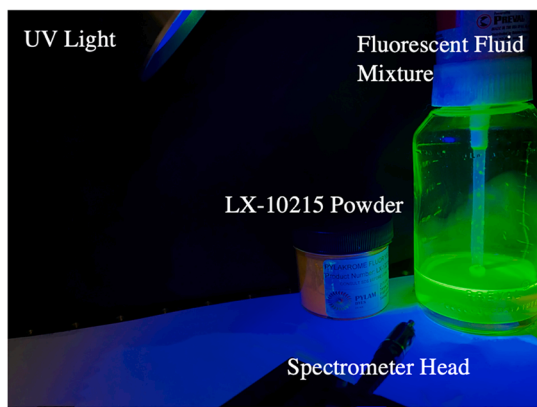


Fig. 1. Fluorescent-reflective fluid fabrication (left) and stokes shift effect (right).

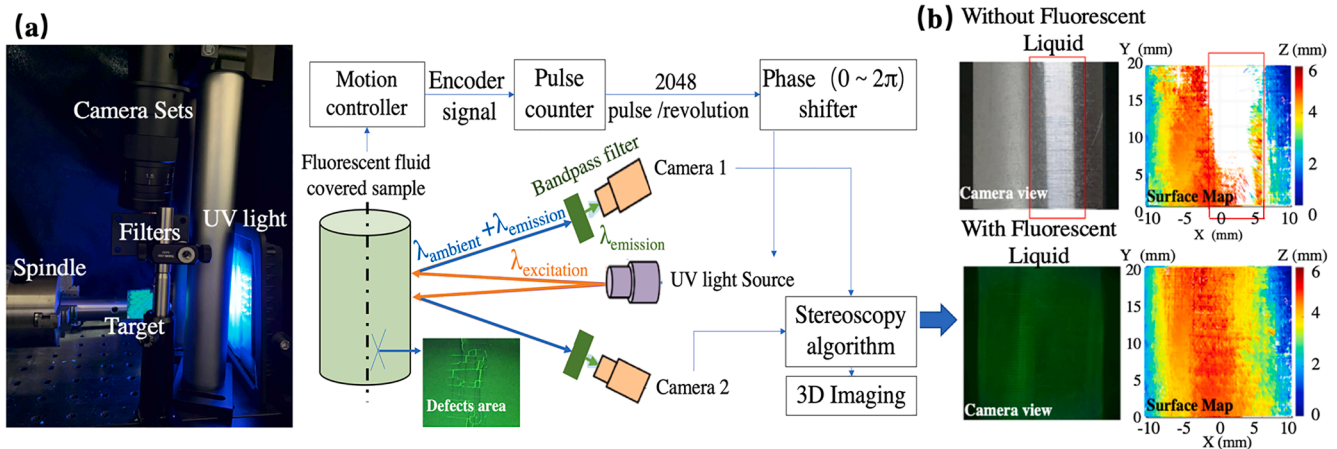


Fig. 2. Principle of fluorescence stroboscopy: (a) experiment set-up and schematic diagram (b) single image reconstruction comparison on an $\phi 1''$ rod under with and without fluorescent fluid conditions.

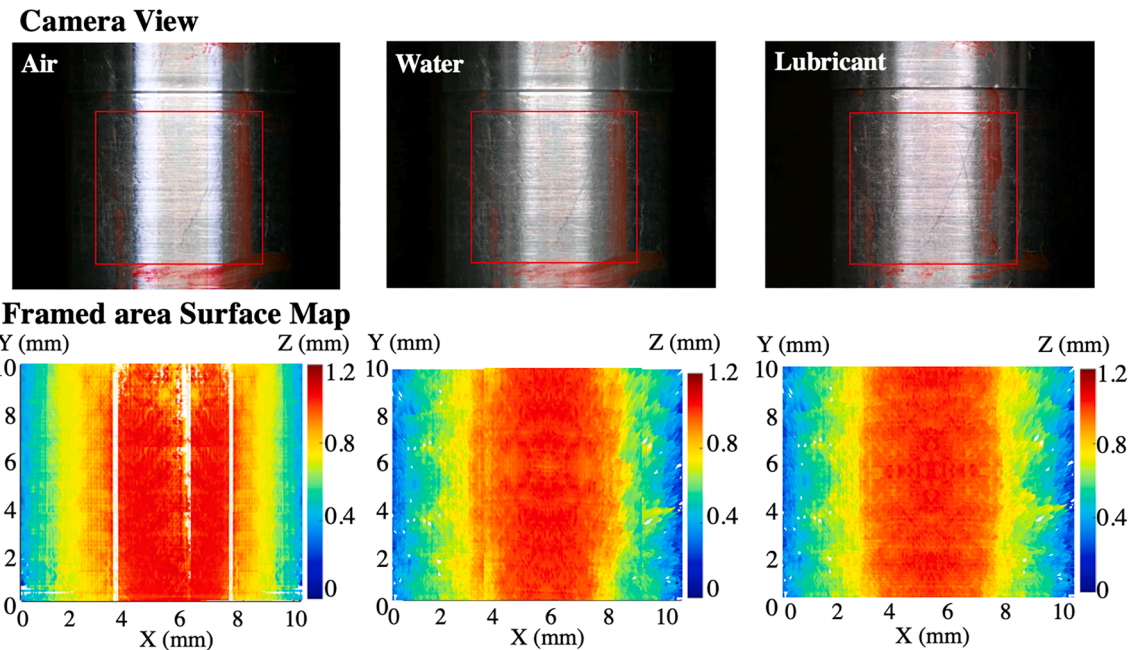


Fig. 3. Fluid media effects on the cylindrical surface.

μm for the normal LED and the fluorescent liquid case, respectively, with the variation of 3.9% variation. Even if the variations are all within 5%, it is difficult for the normal LED condition to perform the complete single image reconstruction.

3.3. FSS on patterned sample

To show the advantage of the use of the fluorescent fluid in eliminating specular reflections and to analyze the performance, a comparison of with and without fluorescent liquid applied surface reconstruction was completed and compared, as is shown in Fig. 5. A flat surface with an aluminum-coated square-patterned structure was selected as a reference target. Though the peak-valley information can be picked up by the reconstructed map, the detected square-patterns are distorted because of the directional specular effect.

A comparative experiment with commercial metrology instruments was conducted to assess the surface reconstruction performance. To confirm the accuracy of the linear scan from the reconstructed surface by the FSS method, a digital microscope, and laser displacement sensor

(LDS, Keyence LK-G35) 1D measurements along the pattern direction were chosen, which are also shown in Fig. 5.

From the results shown above, it can be seen that fluorescent liquid-applied cases can present the pattern clearly. Table 1 compares the average measurement results of two pattern squares in the linear scanned results obtained by the LDS, conventional SS and FSS.

The LDS results are applied as references, and the FSS measured values are more similar. The absolute differences in length are 0.055 mm and 0.11 mm for FSS and SS, respectively, and the difference ratios are 1.4% and 8.1% for each case. Similarly, for the depth situation, the absolute differences are 0.005 mm and 0.03 mm, with 2.3% and 13.9% difference ratios, respectively. The FSS method results are closer to the reference results, and compared with the SS method, it improves 6.7% in the lateral direction and 11.6% in the axial direction.

Furthermore, to prove the capabilities of full cycle 360° 3D target reconstruction, the experiment is performed on an $\phi 2''$ rod with the same patterned structure. The target was fixed on the spindle with a 30 RPM rotating speed. Together, 16 images were taken per cycle (360°) for the stitching process, which means that the pair of cameras captured images

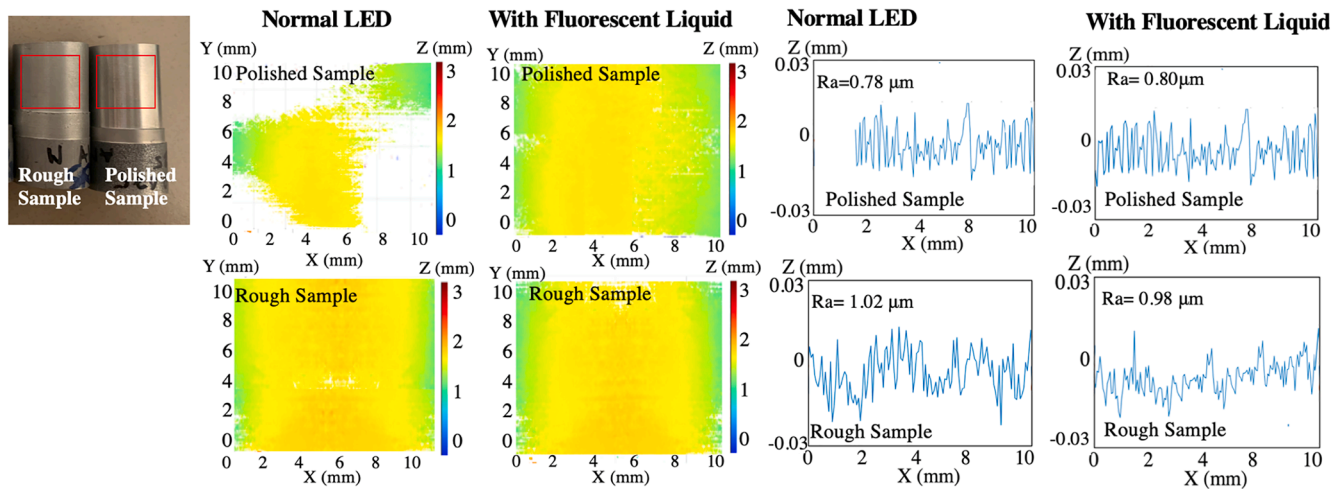


Fig. 4. Imaging results of the normal LED and UV light with fluorescent liquid for rough and polished surface comparison.

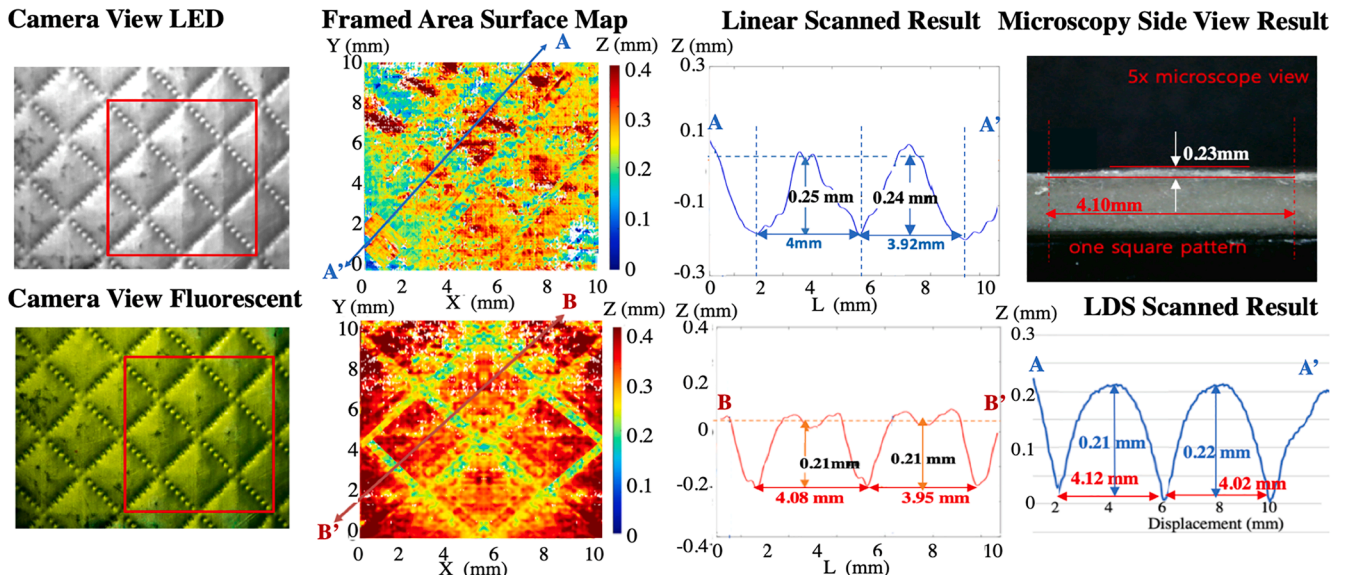


Fig. 5. Comparison of SS and FSS imaging results.

Table 1
Linear scanned comparison results.

	LDS	FSS (with fluorescent fluid)	SS (without fluorescent fluid)
Length (mm)	4.070	4.015	3.96
Depth (mm)	0.215	0.21	0.245

when the spindle rotates every 22.5° . The whole view reconstruction process, along with the FFOV, is in Fig. 6.

The stereoscopic algorithm was first used for single image reconstruction. For convenient neighbor image location stitching, the original curved images were expanded to the tilted images. With the known rotation angle, a phase unwrapping process was applied to generate a tilted stitching map. The panorama surface is gathered following the balancing process, and the 3D full view can eventually be reconstructed. This validates the ability to reconstruct the whole 3D view for cylinder-based targets.

3.4. Dimensional errors

As the whole view reconstruction is achievable, the cylindricity and the roundness error can be analyzed. The FSS process was performed on a reference gauge pin. The results were compared with the CMM measurement analyzed by Zeiss. Together, 5 layers along the z axis were measured to test the cylindricity, which was $1.788 \mu\text{m}$, and each layer's diameter level were also gathered for roundness calculation, which showed that the average deviation was $1.788 \mu\text{m} \pm 0.090 \mu\text{m}$. Fig. 7 shows the FSS whole view reconstructed results, along with the extracted 5 layers top view results. The variation on the cylindricity $2.5 \mu\text{m}$ and the roundness error $2.12 \mu\text{m} \pm 0.166 \mu\text{m}$. The CMM and FSS results showed good agreement in terms of the cylindricity and roundness error.

4. Future work and conclusion

This paper described the measurement principle of FSS and demonstrated that FSS can suppress solid specular reflection, which causes the false reconstruction on the highly reflective surface and provides on-machine FFOV 3D image reconstruction of the rotating part.

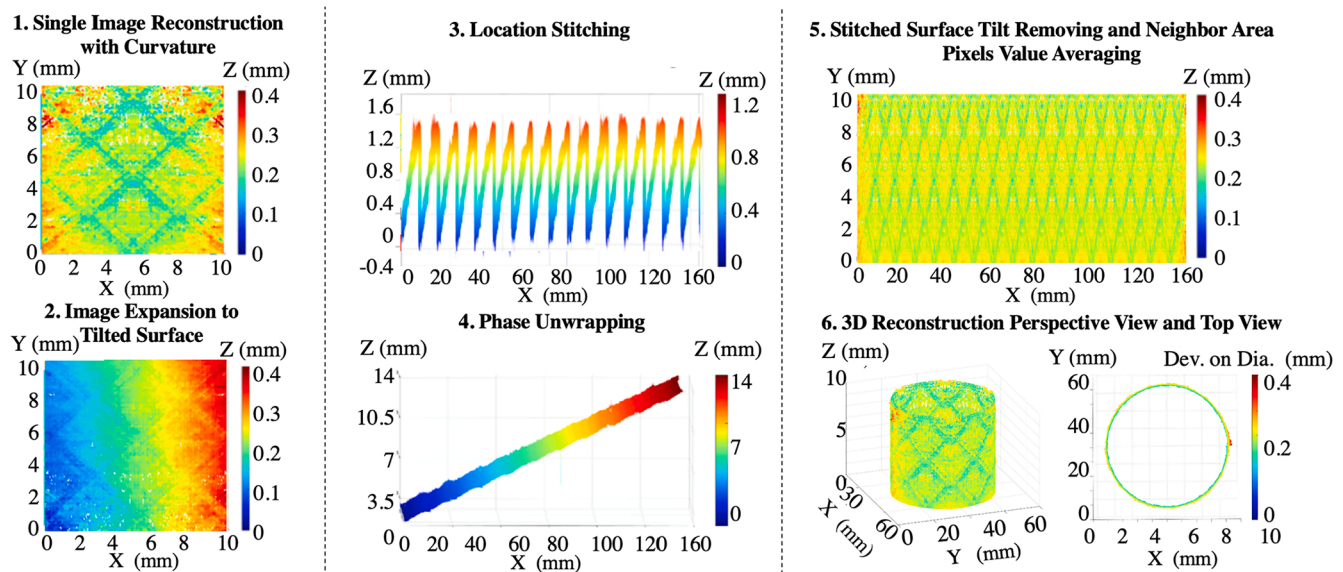


Fig. 6. A full field of 3D FSS image reconstruction process of a target rotating at 30 rpm.

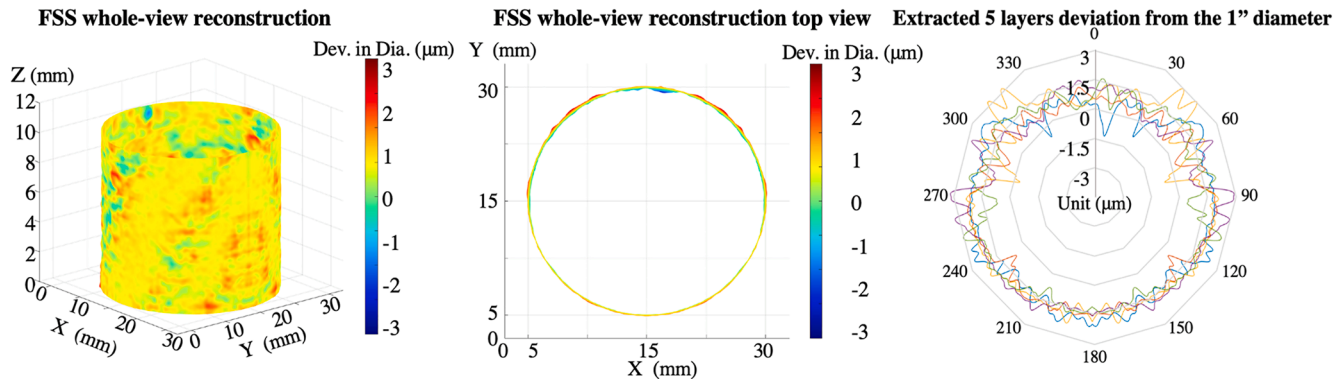


Fig. 7. A full field of 3D FSS image.

The FSS method, as well as the principle of fluorescent liquid implementation, was demonstrated and validated. The comparison experiment of different fluid media demonstrated that higher viscosity liquid giving a better response on the specular reflection suppression. The comparison of the surface quality samples reconstruction proves that the FSS enables 3D surface imaging of the reflective surface in a fast, large-area, low-cost, convenient manner. Based on the aluminum-coated square-patterned surface, the comparison between the flat surface reconstruction with and without fluorescent liquid was performed. For a baseline comparison, CMM, LDS, and the digital microscope were used to compare the variation on the axial and lateral directions. Those differences in the measurement results were only 2.3% and 1.4% for the FSS, respectively, while for those results in the standard white light LED case were 8.1% and 13.9% for the conventional SS. This proves the effectiveness of the fluorescent fluid implementation for high-performance surface imaging. A full view reconstruction of such patterns on the cylinder structure was performed, and the cylindricity and the roundness error were calculated. As a result, the FSS in-process measured FFOV 3D images of the rotating part and analyzed the part features, including the cylindricity and part error.

In the next step, detailed fluorescent fluid experiments, such as multi-emission wavelength effects, target material effects, thin-film generation and related thickness effects, will be performed to investigate the properties of the fluorescent compound. Because the reconstruction resolution is determined not only by the camera parameters,

but also by the fluorescent fluid characteristics, it is possible to develop a solution that can be easily attached to a well-machined specular surface with evenly distributed thin film and higher intensity light for surface information collection and defect detection. Moreover, certain coolant materials are fluorescent by themselves. This technology is expected to be utilized in various manufacturing environments for in-process manufacturing error measurements.

Declaration of Competing Interest

The authors declare that they have no known competing financial interests or personal relationships that could have appeared to influence the work reported in this paper.

Acknowledgments

The research team thanks Honeywell Federal Manufacturing & Technologies LLC for the project (DE-NA0002839), National Science Foundation for the project (Award Number: CMMI 1902697) through the Texas A&M University, and Dr. Bruce Tai at Texas A&M University for the sample preparation and research discussion.

Disclosures

Authors declare no conflicts of interest.

Data availability

Data underlying the results presented in this paper are not publicly available at this time but may be obtained from the authors upon reasonable request.

Significance

This paper introduces a new instrument, the so-called fluorescence strobo-stereoscopy (FSS), and FSS suppresses strong specular reflection and enables the full field of view (FFOV) 3D surface imaging while the part is rotating.

The fluorescent dye-doped fluid applied on the machined surface can be suppressed by separating the fluorescent light from the exciting light.

FSS effectively rejected the specular reflection and improved the FFOV 3D surface image quality of the machined part by enhancing contrast in the rotating target surface. Such enhancements in 3D imaging allowed to identify manufacturing tolerance of the part and to detect the surface features.

The axial and lateral accuracy errors of FSS were 2.3% and 1.4%, respectively. A whole view reconstruction of the cylindrical target sample was performed, and the corresponding cylindricity and diameter deviation were assessed. The fluid media effect and the target surface quality effect were discussed.

FSS in-process measured FFOV 3D images of the rotating part and analyzed the part features, including the cylindricity and part error. This technology is expected to be utilized in various manufacturing environments for manufacturing error measurements.

References

- [1] Yong Bum Seo, Hyo Bin Jeong, Hyug-Gyo Rhee, Young-Sik Ghim, and Ki-Nam Joo, Single-shot freeform surface profiler, *Optics Express*, 28(3), 3401-3409 (2020).
- [2] K. Terzić, M. Hansard, Methods for reducing visual discomfort in stereoscopic 3D: a review, *Signal Process. Image Commun.* 47 (2016) 402-416.
- [3] G.J. Klinker, S.A. Shafer, T. Kanade, The measurement of highlights in color images, *Int. J. Comput. Vision* 2 (1) (1988) 7-32.
- [4] L. Wolff, T. Boult, Constraining object features using a polarization reflectance model, *IEEE Trans. Pattern Anal. Mach. Intell.* 16 (6) (1991) 635-657.
- [5] B.o. Dong, C. Li, B. Pan, Fluorescent digital image correlation applied for macroscale deformation measurement, *Appl. Phys. Lett.* 117 (4) (2020) 044101, <https://doi.org/10.1063/5.0016384>.
- [6] Zhongpai Gao, Alex Hwang, Guangtao Zhai, and Eli Peli, Correcting geometric distortions in stereoscopic 3D imaging, *PLoS ONE* 13(10): e0205032.
- [7] A.V. Gorevoy, A.S. Machikhin, D.D. Khokhlov, V.I. Batshev, Optimization of prism-based stereoscopic imaging systems at the optical design stage with respect to required 3D measurement accuracy, *Opt. Lett.* 28 (17) (2020) 24418-24430.
- [8] D. Shin, B. Javidi, Three-dimensional imaging and visualization of partially occluded objects using axially distributed stereo image sensing, *Opt. Lett.* 37 (9) (2012) 1394-1396.
- [9] D. Abookasis, J. Rosen, Stereoscopic imaging through scattering media, *Opt. Lett.* 31 (6) (2006) 724-726.
- [10] Z. Hu, H. Luo, Y. Du, H. Lu, Fluorescent stereo microscopy for 3D surface profilometry and deformation mapping, *Opt. Express* 21 (2013) 11808-11818.
- [11] T.A. Berfield, H.K. Patel, R.G. Shimmin, P.V. Braun, J. Lambros, N.R. Sottos, Fluorescent image correlation for nanoscale deformation measurements, *Small* 2 (2006) 631-635.
- [12] Z. Hu, T. Xu, H. Luo, R.Z. Gan, H. Lu, Measurement of thickness and profile of a transparent material using fluorescent stereo microscopy, *Opt. Express* 24 (26) (2016) 29822, <https://doi.org/10.1364/OE.24.029822>.
- [13] B.A. Samuel, M.C. Demirel, A. Haque, High resolution deformation and damage detection using fluorescent dyes, *J. Micromech. Microeng.* 17 (2007) 2324-2327.
- [14] X. Guo, ChaBum Lee, Preliminary study of phase-shifting strobo-stereoscopy for cutting tool monitoring, *J. Manuf. Processes* 64 (2021) 1214-1222.
- [15] Surface Texture (Roughness, Waviness, Lay), ASME B46.1-2019 (2020).